Ab initio calculations of the thermodynamic properties of LiF crystal

N. A. Smirnov*

Russian Federal Nuclear Center–Institute of Technical Physics, 456770 Snezhinsk, Russia

(Received 27 October 2010; published 24 January 2011)

This paper presents results obtained in *ab initio* calculations of the thermodynamic properties of B1 and B2 lithium fluoride under pressure. The data were used to calculate LiF isotherms and isochors at pressures from 0 to 500 GPa and temperatures up to the melting point. Calculated results are compared with available theoretical and experimental data on the shock and static compression of LiF crystal. Based on the analysis of our calculations and available experimental data, a hypothetical (P,T) diagram of LiF which includes the crystalline phases B1 and B2 and liquid is proposed.

DOI: 10.1103/PhysRevB.83.014109 PACS number(s): 62.20.de, 62.50.−p, 64.30.Jk

I. INTRODUCTION

Interest in lithium fluoride comes from its wide use in experiments on the shock and static compression of different materials. Lithium fluoride is a chemically stable, optically transparent insulator which melts at a high temperature. It remains transparent when shocked to at least $P \sim 200$ GPa,[1–3] which makes it possible to measure properties of various materials in a wide range of pressures using LiF windows. As shown in Ref. 4, in static measurements on a diamond anvil cell, LiF can be used as a pressure-transmitting medium and a pressure calibrant.

Under ambient conditions LiF has the B1 crystal structure (NaCl type). The structure remains unchanged under pressures up to ∼100 GPa and temperatures to the melting point.[4,5] The elastic properties of LiF at ambient pressure were investigated in considerable detail in a number of papers under both low and high temperatures.[6–9] Its equation of state was investigated in static experiments at temperatures from room temperature to ∼1000 K and pressures up to 37 GPa in Refs. 4 and 10–12. LiF crystals were actively studied in shock experiments too.[1–3,13–16] LiF shock compression to ∼485 GPa was studied in Refs. 14 and 15. Using data from these experiments it was determined that LiF melts under shock compression at $P_m = 280$ GPa, $T_m = 6000$ K.[15] It should be noted that these values correspond to the end of the melting of shocked LiF. The point[15] markedly disagrees with the melting curve measured in diamond anvil experiments.[5] As shown in Ref. 17 with the molecular dynamics (MD) simulation, this disagreement can be removed if a B1 → B2 (CsCl type) structural transition is allowed to occur in LiF.

In contrast to experimental investigations, calculations of LiF properties, especially under pressure, are rather few. The papers in Refs. 18–20 investigate the electronic structure and properties of LiF in its ground state using the Hartree-Fock method and the density-functional approach in a local-density approximation. The optical properties of shocked LiF were studied with *ab initio* MD in Ref. 21. A melting curve with the structural transition B1 → B2 under pressure was calculated with classical MD in Ref. 17. Results of that work allow removal of the previously mentioned discrepancy in the determination of the melting curve in different experiments.

Here we describe *ab initio* full-potential linear muffin-tin orbital (FP-LMTO) calculations taken to obtain elastic constants and a number of thermodynamic properties of LiF in a wide range of pressures, which will help us more completely and accurately describe the processes that occur in LiF under pressure. We investigate two LiF modifications: B1 and B2. We also study the possibility of the structural B1 → B2 transition under pressure. Calculated and experimental results were used to construct a hypothetical (P,T) diagram of LiF which includes B1 and B2 structures and liquid.

II. CALCULATION METHOD

The dependence of specific energy on volume and cell shape at $T = 0$ K was calculated with the full-potential linear muffin-tin orbital method[22] (the LMTART code package[23] with a few modifications[24]). Lithium fluoride was investigated at compressions ϱ/ϱ_0 from 0.909 to 3.333. Hereafter $\varrho_0 = 1/V_0$ is LiF density at ambient pressure and $T = 300$ K; here $V_0 = 55.04$ a.u./atom is the specific volume from experiment.[25] Pressure was found through numerical differentiation of specific energy vs volume.

In our calculations, only 1*s* electrons of the fluorine atom were treated as core electrons; all the rest were valence electrons. All electrons of Li were treated as valence electrons. The Barth-Hedin functional[26] with gradient corrections[27] was used to calculate the exchange-correlation energy. To ensure high accuracy of the calculated specific energy, we thoroughly selected parameters of the method proposed in Ref. 22. For both lithium and fluorine, the *s*, *p*, and *d* functions were included in the basis of the wave-function representation ($l^b_{\max} = 2$); in potential and charge density expansions we used $l^w_{\max} = 6$; and in the reexpansion of basis functions $l^\tau_{\max} = 6$. For each element, eight linearization centers and three tail energies were taken in accord with the algorithm described in Ref. 24. For the representation of the *s*, *p*, and *d* basis functions in the interstitial region, we used the same number of plane waves: about 2420 (cutoff energy 110 Ry). This value slightly changed when the shape of the unit cell changed, but was always greater than 2000. A mesh of size (30,30,30) was used for the fast Fourier transform. The mesh for integration in reciprocal space with the linear tetrahedron method[28] was constructed in the prism-shaped Brillouin zone by dividing each edge into the same number of sections, $n_k = 10$.

Elastic constants were calculated from the second derivatives of the specific energy with respect to chosen strains. A detailed description of the method we used here

TABLE I. Calculated V_0, B_0, B_0', C', C_{44}, and Θ_D for B1 LiF in comparison with experimental data (RT denotes room temperature experiment).

	Calculation $T = 0$ K	Experiment
V_0 (a.u./atom)	54.90	55.04,[25] 55.48[4] (RT)
B_0 (GPa)	73.8	73.0[4] (RT)
B_0'	3.76	3.90[4] (RT)
C' (GPa)	41.3	41.1[6] ($T = 0$ K)
C_{44} (GPa)	66.0	64.9[6] ($T = 0$ K)
Θ_D (K)	736	734[6] ($T = 0$ K)

to calculate elastic constants under pressure can be found in Ref. 29. The thermal motion of nuclei was considered with the modified Debye model described in Ref. 30. In that model its contribution to thermodynamic functions is expressed with only one parameter: Debye temperature Θ_D that is defined by the mean sound velocity in the crystal[31] and depends only on volume. The mean sound velocity can be found from the elastic constants.[30]

III. RESULTS

To verify accuracy of our calculations, we first calculated a number of parameters for LiF at ambient pressure and zero temperature and then compared them with available experimental data. The parameters included specific volume V_0, bulk modulus B_0 and its pressure derivative B_0', elastic constants $C' = (C_{11} - C_{12})/2$ and C_{44}, and Debye temperature Θ_D for the structure B1 of LiF at $P = 0$ and $T = 0$ K. Table I compares calculated and experimental results. It is seen that the values we obtained in calculations agree well with the experimental ones, which proves that our calculations are rather accurate.

Then we calculated specific energy vs compression for the B1 and B2 structures at $T = 0$ K and $\varrho/\varrho_0 = 0.909 \div 3.333$. The cold pressure for both structures was calculated through the numerical differentiation of energy. With the resulted energies and pressures, we determined Gibbs potentials $G = E + PV$ for the B1 and B2 structures at zero temperature. Figure 1 shows these potentials plotted relative to the Gibbs potential of the B1 structure. It is seen from Fig. 1 that at $T = 0$ K, the B1 structure is more thermodynamically stable in the entire pressure range from 0 to 1000 GPa. At pressures above ~100 GPa, the difference between B1 and B2 potentials only grows. The band gap of the B1 structure at $P = 0$, $T = 0$ K, was calculated to be ~9 eV, which agrees well with the value calculated in Ref. 21 and is about 30% lower than the experimental 13.6 eV.[32] Our calculations show that under pressures up to 1000 GPa and temperature 0 K, the two lithium fluoride structures (B1 and B2) maintain a good dielectric with a band gap larger than 9 eV.

Further, we calculated elastic constants for B1 and B2 LiF at $T = 0$ K. Figure 2 shows the dependence of the elastic constants C' and C_{44} on compression. The B1 structure is seen to be mechanically stable in the entire range of compressions; its elastic constants are monotonically increasing. The B2

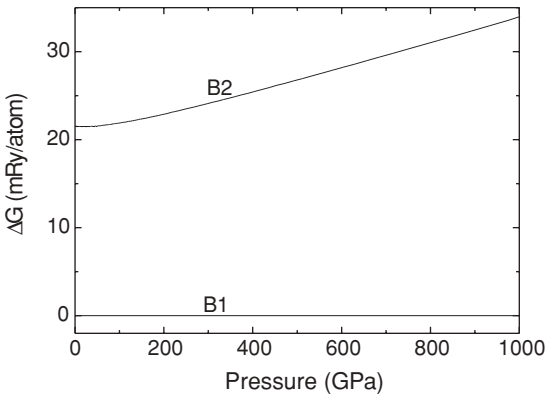

FIG. 1. Gibbs potential difference $\Delta G = G_{B2} - G_{B1}$ vs pressure at $T = 0$ K for considered structures of LiF (the contribution of zero-point vibrations is not taken into account).

structure, in turn, is mechanically unstable at $\varrho/\varrho_0 < 1.6$ ($P < 90$ GPa) relative to the shear deformation which defines C_{44}. The values of C_{11}, C_{12}, and C_{44}, calculated in this work, are presented in Table II for structures B1 and B2.

Figure 3 shows isotherms 300 K and 985 K calculated for the B1 structure in comparison with experimental data.[4] This figure also depicts the cold curve for LiF ($T = 0$ K). The isotherms are seen to agree well with experiment. A minor overestimation of pressure on the isotherms is almost identical for both considered cases.

We also calculated LiF Hugoniots in (P,T) and $(P,\varrho/\varrho_0)$ coordinates. Figure 4 shows the Hugoniot of the B1 structure in (P,T) coordinates along with similar data obtained with the *ab initio* MD method[21] and available experimental data.[15] The curve is seen to agree well with MD calculations[21] and with data from Ref. 15 that were obtained through treatment experimental data with the Mie-Grüneisen equation of state.

Figure 5 presents the Hugoniot in $(P,\varrho/\varrho_0)$ coordinates. Closed circles show the experimental points from Refs. 14 and 34 that correspond, in their authors' view, to the liquid phase of LiF. It is seen from the figure that the Hugoniot agrees well with experiment at compressions below $\varrho/\varrho_0 \approx 1.6$ ($P \approx 110$ GPa). At higher compressions, the deviation of the experimental points[14,34] from our curve and from points

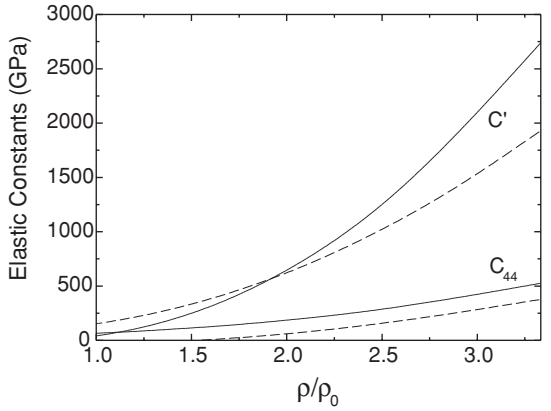

FIG. 2. Calculated elastic constants vs compression for the B1 (solid line) and B2 (dashed line) structures of lithium fluoride at $T = 0$ K.

TABLE II. Values of C_{11}, C_{12}, C_{44}, and pressure P (in GPa) from our calculations for the B1 and B2 structures at different specific volumes and $T = 0$ K.

ϱ_0/ϱ	C_{11}	C_{12}	C_{44}	P
		B1 structure		
1.10	74.832	33.310	62.715	−5.868
1.05	98.643	38.958	63.834	−3.408
1.00	127.38	45.947	65.803	−0.186
0.95	162.86	53.332	69.688	3.9594
0.90	207.70	62.861	74.632	9.3857
0.80	335.95	89.168	87.434	25.802
0.70	548.63	131.23	106.06	54.830
0.60	921.87	202.82	135.29	108.74
0.50	1627.0	334.24	185.48	216.25
0.40	3105.3	601.82	287.42	454.24
0.30	6657.2	1178.5	525.91	1071.6
		B2 structure		
1.10	217.78	−38.33	−29.22	−5.971
1.00	276.31	−28.79	−29.53	−0.314
0.90	356.66	−10.49	−25.73	9.2935
0.80	480.63	20.051	−19.99	25.868
0.70	677.80	74.331	−8.500	55.370
0.60	1010.7	175.03	14.579	110.49
0.55	1266.1	257.06	32.965	155.74
0.50	1618.6	374.61	60.034	221.12
0.45	2119.0	547.64	99.289	318.26
0.40	2854.6	810.37	156.93	467.60
0.35	3974.3	1224.0	244.80	707.97
0.30	5724.4	1863.8	376.75	1112.0

obtained in Ref. 21 becomes noticeable. Calculations systematically overestimate values of the pressure between $\varrho/\varrho_0 \approx 1.7$ and $\varrho/\varrho_0 \approx 1.95$. According to data from Refs. 14 and 15, at pressures below ∼250 GPa ($\varrho/\varrho_0 < 1.95$) lithium fluoride is still in a crystalline state and does not melt. Moreover, when a strongly compressed material melts, significant deviation of the Hugoniot is not usually observed,[35] which is also seen in Fig. 5. But, as shown in Ref. 35, for example, in the case of Fe and KCl, polymorphous transitions often cause breaks in Hugoniots. As mentioned in Refs. 14 and 17, the polymorphic B1 → B2 transition may occur in LiF under high pressures and temperatures.

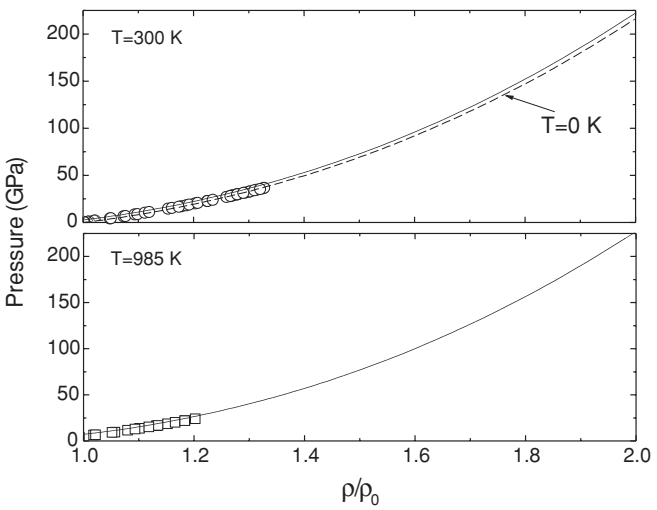

FIG. 3. Isotherms 300 K and 985 K for the B1 structure obtained in calculation (solid line) and in static experiment (Ref. 4): circles, $T = 300$ K; squares, experimental data for temperatures 980–990 K. The dashed line shows calculation at $T = 0$ K without zero-point oscillations.

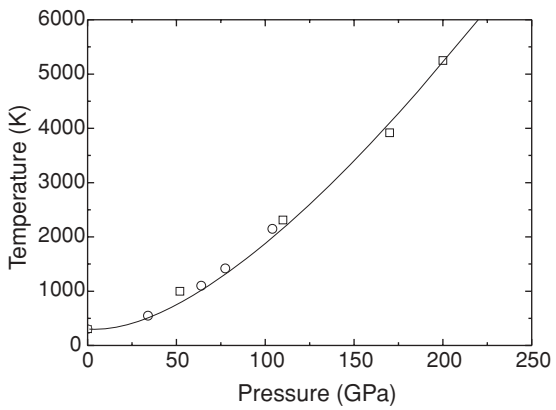

FIG. 4. LiF Hugoniot in (P,T) coordinates: The solid line shows our calculation for the B1 structure; □, results of *ab initio* MD calculations for the B1 structure (Ref. 21); and ○, results obtained from the processing of experiment (Ref. 15).

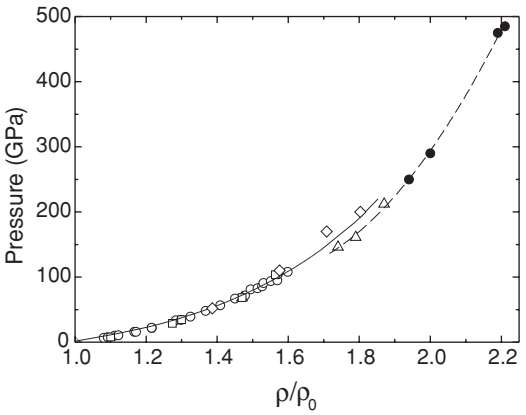

FIG. 5. LiF Hugoniot in $(P,\varrho/\varrho_0)$ coordinates: The solid line shows our calculation for the B1 structure; ◇, *ab initio* MD calculations for the B1 structure (Ref. 21); □, experiment (Ref. 13); △, experiment (Ref. 14); ○, experiment (Ref. 33); ●, experimental points from Refs. 14 and 34 that correspond, in the authors' view, to the liquid phase of LiF. The dashed line is the parabolic approximation of experimental points at $\varrho/\varrho_0 > 1.7$.

To estimate the possibility of the structural B1 → B2 transition in lithium fluoride under pressure and nonzero temperature, we determined the interface of these structures in (P,T) coordinates. Figure 6 presents the B1-B2 phase boundary together with available experimental data on the melting curve of LiF.[5,15] The solid line shows the B1-B2 interface and the dotted one shows the boundary of a region where the B2 structure is mechanically stable in our calculations. The boundary of mechanical stability was evaluated from the relation $V_{B2}(P,T) = V_b$, where V_b is the specific volume at which $C_{44} = 0$ at $T = 0$ K. Our thermodynamic model is not sufficiently accurate near this boundary because of our not accounting for the variation of elastic constants with temperature in the region where material loses mechanical stability. The dashed line in Fig. 6 shows the Hugoniot of the structure B1 from our calculations.

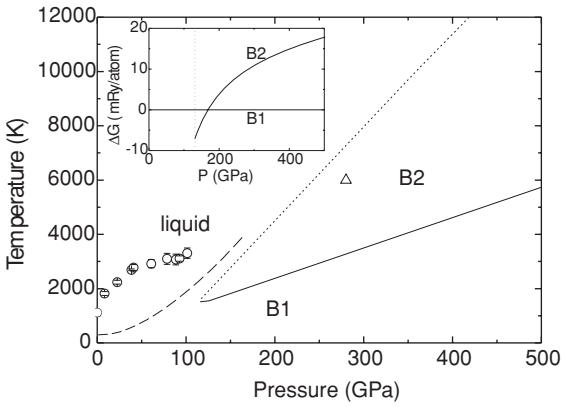

FIG. 6. B1-B2 phase boundary (solid line) and B1 Hugoniot (dashed line) from our calculations. Here ○ shows the melting curve from experiment (Ref. 5) and △ shows the experimental shock melting point from Ref. 15. The insertion shows Gibbs potential difference ΔG vs pressure at $T = 2000$ K for B1 and B2 LiF. The dotted line shows the boundary of mechanical stability of the structure B2.

As seen from Fig. 6, there is a region on the (P,T) diagram where the B2 structure is more thermodynamically favored than the B1 structure. A part of this region is below the experimental melting curve. At temperatures below ∼1500 K, the B1 structure is thermodynamically favored in the entire range of pressures under consideration. However, when temperatures become higher than 1500 K and at pressures above 100 GPa, the structural B1 → B2 transition occurs in LiF. At high compressions, the elastic constants of the B2 structure are softer (Fig. 2) and its Debye temperature is therefore lower. In Fig. 7 solid lines show Debye temperatures we calculated for the B1 and B2 structures at $T = 0$ K. The difference in Θ_D is seen to be rather large in the entire range of compressions. For $\varrho/\varrho_0 = 3.333$, it equals ∼400 K.

Unfortunately, since the B2 structure is mechanically unstable at $\varrho/\varrho_0 < 1.6$ and zero temperature, we cannot determine Θ_D for it and obtain thermodynamic functions with the thermodynamic model from Ref. 30. It is also quite evident that temperature must be of effect on the elastic constants and Debye temperature.[7–9] Furthermore, it seems quite possible that the B2 structure stabilizes at low compressions and $T > 0$ K, as it happens with, for example, bcc titanium.[36,37] All this is not considered in our thermodynamic model. Nevertheless, using available experimental and theoretical results, we can construct a hypothetical (P,T) diagram of LiF if we correct (within calculation accuracy) calculated compression dependencies of Debye temperatures at $T > 1100$ K, as shown in Fig. 7.

In order to correct $\Theta_D(\varrho/\varrho_0)$ for the B1 structure, we used experimental data from Refs. 7–9 on the temperature dependence of elastic constants, and data from Ref. 38 on the temperature expansion of LiF at ambient pressure. The extrapolation estimate of Θ_D at $T = 1100$ K and $\varrho/\varrho_0 = 0.886$ we obtained using Refs. 7 and 38 equals ∼460 K. The values of Θ_D calculated from different experimental results[7–9] differ by no more than 10% at $T = 1100$ K. Also, it seems quite reasonable to assume that the effect of temperature on Θ_D will weaken as compression grows. Therefore, the curves $\Theta_D(\varrho/\varrho_0)$ for zero and nonzero temperatures must get closer

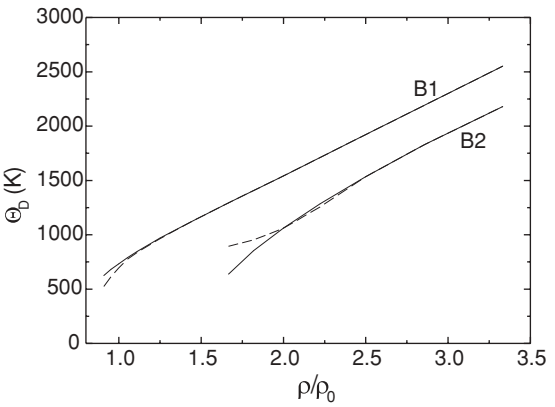

FIG. 7. Calculated Debye temperatures for the B1 and B2 structures of lithium fluoride: the solid lines show Θ_D at $= 0$ K and the dashed ones show the Θ_D corrected for high temperatures ($T > 1100$ K, see text).

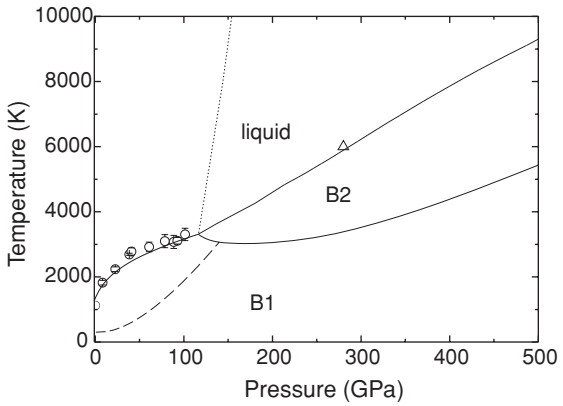

FIG. 8. A hypothetical phase diagram of lithium fluoride: The solid line shows the calculated diagram, the dashed one shows the calculated Hugoniot, and the dotted line shows the boundary of mechanical stability of the structure B2. Here ○ shows the melting curve by data from experiment (Ref. 5) and △ shows the experimental shock melting point from Ref. 15.

during compression (Fig. 7). In order to correct Θ_D for the B2 structure, we used experimental data from Ref. 14, having assumed that Hugoniot points (Fig. 5) at $1.6 < \varrho/\varrho_0 < 1.9$ correspond to the B2 structure. The dependence $\Theta_D(\varrho/\varrho_0)$ was taken to be such as to reproduce the experimental Hugoniot at $\varrho/\varrho_0 > 1.6$.[14] The new curve $\Theta_D(\varrho/\varrho_0)$ obtained for the B2 structure is shown in Fig. 7.

Figure 8 presents a hypothetical phase diagram of lithium fluoride which was constructed using the corrected Debye temperatures. Here the solid line shows phase boundaries, the dashed line shows the Hugoniot calculated for the B1 structure, and the dotted one shows the boundary of mechanical stability of the B2 structure which is now above the melting curve. The melting curve was obtained through fitting experimental data to the Lindeman formula, $T_m(V) = CV^{2/3}\Theta_D^2(V)$, where $\Theta_D(V)$ is the corrected dependence of Debye temperature on volume ($C = 1.89 \times 10^{-4}$). It is seen from Fig. 8 that the calculated melting curve agrees well with experimental

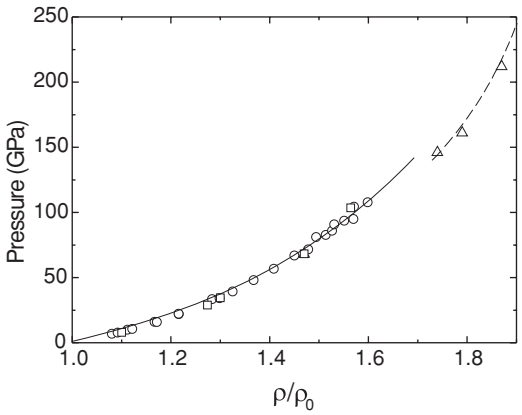

FIG. 9. Lithium fluoride Hugoniot: the solid and dashed lines show the Hugoniots calculated for the B1 and B2 structures, respectively, with the dependencies $\Theta_D(\varrho/\varrho_0)$ corrected for high temperature (see text). Experiment: □ (Ref. 13), △ (Ref. 14), ○ (Ref. 33).

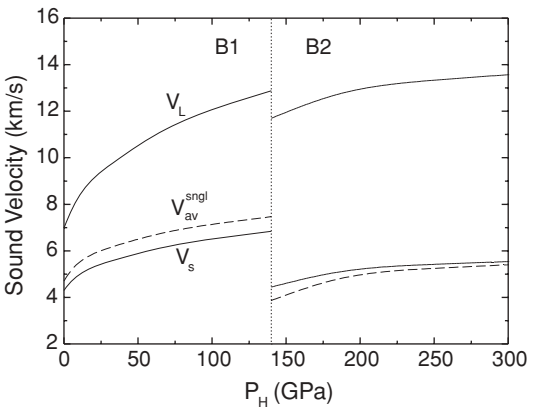

FIG. 10. Estimated longitudinal V_p and transverse V_s sound velocities versus pressure on the Hugoniot in polycrystal LiF (the solid lines) and mean sound velocity $V_{\rm av}^{\rm sngl}$ in single-crystal LiF (the dashed line) with the structural B1 → B2 transition. The dotted line shows a pressure on the Hugoniot at which the transition occurs in our calculations.

data. The presence of the B2 structure at high pressures and temperatures allows us to bring melting curves from static and shock experiments into agreement. A similar result was obtained in MD calculations.[17] The Hugoniot crosses the B1-B2 phase boundary at $P \approx 140$ GPa and $T \approx 3100$ K. Figure 9 shows the calculated Hugoniot in $(P, \varrho/\varrho_0)$ coordinates with the structural B1 → B2 transition. The change in volume is about 2.5% at this transition.

Confirming that the structural transition on the LiF Hugoniot is possible requires further calculations, taking into account the lack of our thermodynamic model[30] and experiments. The most useful here could be experiments for sound velocity in shock-compressed LiF at $P > 100$ GPa. The estimated dependence of sound velocity on pressure on the Hugoniot with account for the structural B1 → B2 transition is shown in Fig. 10. Here V_p and V_s are longitudinal and transverse sound velocities in polycrystal LiF, determined with the code,[39] and $V_{\rm av}^{\rm sngl}$ is a mean sound velocity in single-crystal LiF.[31] All the velocities we calculated are seen to noticeably change in values on the boundary of the structural B1 → B2 transition and therefore can be observed in experiment. It should also be noted that the transition is accompanied by the lowering of sound velocities V_p and V_s in polycrystal and $V_{\rm av}^{\rm sngl}$ in single-crystal LiF.

IV. CONCLUSION

This paper has presented elastic and some thermodynamic properties of the crystalline structures B1 and B2 of lithium fluoride, obtained in *ab initio* calculations. The calculated elastic constants, isotherms, and Hugoniot agree well with experiment. A hypothetical (P,T) diagram of LiF in a wide range of pressures and temperatures was constructed with the use of available calculated and experimental data. It is shown that the B2 structure is more thermodynamically favored at $P > 100$ GPa and $T > 1500$ K. The pressure and temperature at which the Hugoniot crosses the boundary

between the structures B1 and B2 were estimated to be $P \approx 140$ GPa and $T \approx 3100$ K. It was also evaluated how the velocity of sound on the Hugoniot changes in the presence of the B1 → B2 transition in polycrystal and single-crystal LiF. The change in the sound velocity must be more than 10%.

ACKNOWLEDGMENTS

The author expresses gratitude to Dr. G.V. Sin'ko for useful discussions of the results of the present work. This work was supported by the Russian Foundation for Basic Research (Grant 08-08-01055).

*deldavis@mail.ru

[1] J. S. Wise and L. Ñ. Chhabildas, in *Shock Wave in Condensed Matter*, edited by Y. M. Gupta (Plenum, New York, 1986), p. 441.
[2] G. Huser, M. Koenig, A. Benuzzi-Mounaix, E. Henry, T. Vinci, B. Faral, M. Tomasini, B. Telaro, and D. Batani, Phys. Plasmas **10**, L61 (2004).
[3] M. D. Furnish, L. C. Chhabildas, and W. D. Reinhart, Int. J. Imp. Eng. **23**, 261 (1999).
[4] J. Liu, L. Dubrovinsky, T. B. Ballaran, and W. Crichton, High Press. Res. **27**, 483 (2007).
[5] R. Boehler, M. Ross, and D. B. Boercker, Phys. Rev. Lett. **78**, 4589 (1997).
[6] C. V. Briscoe and C. F. Squire, Phys. Rev. **106**, 1175 (1957).
[7] Yu. M. Chernov and A. V. Stepanov, Fiz. Tverd. Tela **3**, 2872 (1961) [Sov. Phys. Solid State **3**, 2097 (1962)].
[8] L. E. A. Jones, Phys. Earth Planet. Inter. **13**, 105 (1976).
[9] S. Hart, J. Phys. D: Appl. Phys. **10**, L261 (1977).
[10] M. Pagannone and H. G. Drickamer, J. Chem. Phys. **43**, 2266 (1965).
[11] K. Y. Kim, L. C. Chhabildas, and A. L. Ruoff, J. Appl. Phys. **47**, 2862 (1976).
[12] T. Yagi, J. Phys. Chem. Solids **39**, 563 (1978).
[13] L. V. Al'tshuler, M. N. Pavlovskii, L. V. Kuleshova, and G. V. Simakov, Fiz. Tverd. Tela **5**, 279 (1963) [Sov. Phys. Solid State **5**, 203 (1963)].
[14] S. B. Kormer, M. V. Sinitsin, A. I. Funtikov, V. D. Urlin, A. V. Blinov, Zh. Eksp. Teor. Fiz. **47**, 1202 (1964) [Sov. Phys. JETP **20**, 811 (1965)].
[15] S. B. Kormer, Sov. Phys. Usp. **11**, 229 (1968).
[16] D. G. Hicks, P. M. Celliers, G. W. Collins, J. H. Eggert, and S. J. Moon, Phys. Rev. Lett. **91**, 035502 (2003).
[17] A. B. Belonoshko, R. Ahuja, and B. Johansson, Phys. Rev. B **61**, 11928 (2000).
[18] A. Zunger and A. J. Freeman, Phys. Rev. B **16**, 2901 (1977).
[19] A. B. Kunz, Phys. Rev. B **26**, 2056 (1982).
[20] K. Doll and H. Stoll, Phys. Rev. B **56**, 10121 (1997).
[21] J. Clerouin, Y. Laudernet, V. Recoules, and S. Mazevet, Phys. Rev. B **72**, 155122 (2005).
[22] S. Yu. Savrasov, Phys. Rev. B **54**, 16470 (1996).
[23] [http://physics.ucdavis.edu/∼savrasov/.]
[24] G. V. Sin'ko and N. A. Smirnov, Phys. Rev. B **74**, 134113 (2006).
[25] H.-J. Ullrich, A. Uhlig, G. Geise, H. Horn, and H. Waltinger, Mikrochim. Acta **107**, 283 (1992).
[26] U.von Barth and L. Hedin, J. Phys. C **5**, 1629 (1972).
[27] J. P. Perdew, K. Burke, and M. Ernzerhof, Phys. Rev. Lett. **77**, 3865 (1996); **78**, 1396(E) (1997).
[28] P. E. Blochl, O. Jepsen, and O. K. Andersen, Phys. Rev. B **49**, 16223 (1994).
[29] G. V. Sin'ko, Phys. Rev. B **77**, 104118 (2008).
[30] G. V. Sin'ko and N. A. Smirnov, J. Phys. Condens. Matter **14**, 6989 (2002).
[31] N. W. Ashcroft and N. D. Mermin, *Solid State Physics* (Holt, Rinehart and Winston, New York, 1976).
[32] D. M. Roessler and W. C. Walker, J. Phys. Chem. Solids **28**, 1507 (1967).
[33] *Los Alamos Shock Hugoniot Data*, edited by S. P. Marsh (University of California Press, Berkeley, CA, 1980).
[34] S. B. Kormer, M. V. Sinitsyn, and A. I. Kuryapin, Zh. Eksp. Teor. Fiz. **55**, 1626 (1968) [Sov. Phys. JETP **28**, 852 (1969)].
[35] *Methods to Investigate Material Properties Under Intense Dynamic Loads*, edited by M.V. Zhernokletov (RFNC-VNIIEF, Sarov, 2005).
[36] W. Petry, A. Heiming, J. Trampenau, M. Alba, C. Herzig, H. R. Schober, and G. Vogl, Phys. Rev. B **43**, 10933 (1991).
[37] K. Persson, M. Ekman, and V. Ozolins, Phys. Rev. B **61**, 11221 (2000).
[38] K. K. Srivastava and H. D. Merchant, J. Phys. Chem. Solids **34**, 2069 (1973).
[39] J. P. Watt, Comput. Geosci. **13**, 441 (1987).